Desalination and Water Treatment
www.deswater.com

doi:10.5004/dwt.2018.22479

116 (2018) 284–293
June

Study of the kinetic model and the degradation process of the treatment of dye simulated wastewater using a coupled bio-electrochemical AF-BAF

Ajun Wan, Yixuan Xie, Luting Pan*, Xinjun Xie, Houzhang Zhou, Guijiao Lin

National Engineering Research Center of Protected Agriculture, Modern Agricultural Science and Engineering Institute, Tongji University, Shanghai 200092, China, email: wanajun@tongji.edu.cn (A. Wan), 1620071611@qq.com (Y. Xie), Tel. +02159548507, email: lutingpan@163.com (L.T. Pan), jane_xiexinjue@163.com (X. Xie), zhouhzv@163.com (H. Zhou), lgj1310476223@163.com (G. Lin)

Received 6 September 2017; Accepted 7 May 2018

ABSTRACT

Experiments were performed to investigate the mechanism of a biological anaerobic filter-biological aerobic filter (AF-BAF) process coupled with internal electrolysis for the treatment of dye simulated wastewater containing reactive brilliant red X-3B dye. A kinetic model of the anaerobic reactor was set up to provide the dependence of the COD removal rate on organic substrates (first-order) and the decolourization rate on dye concentration (first-order). Moreover, the results of gas chromatography/mass spectrum (GC-MS) and UV-visible spectrophotometer (UV-Vis) analyses demonstrated that azo chromophore side groups were destroyed and the degradation of benzene and naphthalene ring intermediates was intensified in the anaerobic stage by the coupled bio-electrochemical AF-BAF process. Additionally, the remaining benzene ring derivatives were further degraded by the subsequent aerobic stage.

Keywords: Coupling system of electrochemistry and biochemistry; Kinetic model; Reactive brilliant red X-3B; Dyeing wastewater

1. Introduction

Dyeing Wastewater (DW) is one form of refractory industrial wastewater because it involves the consumption of a huge amount of water, has a complex composition, is of high chromaticity, contains many refractory substances contained, and is of low biodegradability, among other characteristics [1]. At present, physicochemical and biological processes [2] have been explored for the treatment of actual DW. However, compared with the physical and chemical methods, the biological method is more commonly used because of it high economic efficiency. The biological method utilized for the actual DW is mainly the anaerobic–aerobic combination process; however, this process has some shortcomings [3], such as the instability of the removal of aniline compounds, and poor load resistance.

Iron-carbon inner electrolysis is the treatment of wastewater with based on the principle of electrochemical corrosion of metals. Iron and carbon particles can form the primary batteries, that provide the strong reducing ability of [H] and iron ions and the strong oxidizing ability of [OH] free radicals for decomposing organic compounds in wastewater to realize open loops and broken chains of macromolecules thereby allowing biodegradability of wastewater to be strengthened to facilitate the subsequent biochemical reaction. Therefore, in recent years much attention has been focused on the internal electrolysis coupled anaerobic treatment for DW [4].Compared with the conventional biochemical treatment, the coupled process can remove pollutants at a low organic concentration for a short time and reduce microbial dependence on symbiotic metabolism. The main advantage of the coupled system is that it produces less aromatic amine intermediates. In the previous research, the micro-electrolysis coupling process has provided satisfactory results; however, the existing research has not analysed the degradation process of organic compounds in the coupled system and has not revealed the mechanism of the coupled system.

*Corresponding author.

In this experiment, reactive brilliant red X-3B simulated DW was taken as the research object to study the wastewater treatment performance of the AF-BAF combined process with built-in internal electrolytic packings. Through laboratory simulation, the following were deeply investigated: the degradation of the pollutants caused by the coupling reactor in the anaerobic segment, the kinetics of the organic substrates and dye degradation, and the kinetic parameters in the anaerobic coupled reactor. The process of dye degradation and the mechanism of the coupled system were also explored. The results have important significance for understanding the characteristics of dye degradation via the internal electrolysis coupled biological process, and provide a theoretical and design basis for practical application.

2. Experiments

2.1. Experimental water

The molecular structure of reactive brilliant red X-3B is shown in Fig. 1. In this test, the reactive brilliant red X-3B azo dye wastewater was taken as the research object because it is a widely used azo dye. This test dyestuff with the purity is 99% was taken from Shanghai Jia Ying Chemical Co., Ltd. The stimulated wastewater samples used in this experiment were prepared artificially, with $C_6H_{12}O_6$, NH_4Cl and KH_2PO_4 added in proportion (concentration ratio of C:N:P = 200:5:1) as the carbon, nitrogen and phosphorus source of the influent, respectively. $NaHCO_3$ and H_2SO_4 were chosen as the acidity regulator to adjust the influent pH value. Moreover, 0.3 ml of nutrient solution was added to each litre of stimulated wastewater influent [5].

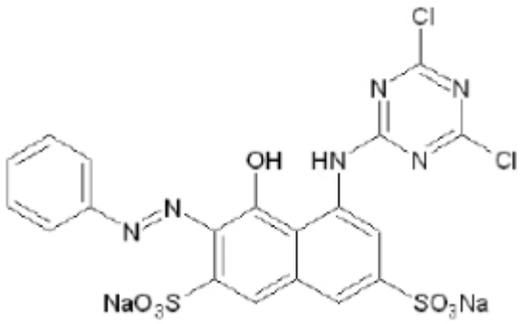

Fig. 1. The chemical structure of reactive brilliant red X-3B.

2.2 Apparatus and experimental procedures

In this experiment, the internal electrolysis packing was positioned in the anaerobic and aerobic reactor. Simulated DW was treated by an electrochemical coupled AF-BAF two-stage biological filter system. The new type of iron carbon composite filler used in the test is a technical product developed by our research group [Application Number:200910198816.9]. These fillers are composed of a certain mass ratio of iron powder and activated carbon powder, as along with a small amount of binder and catalyst.

The experimental apparatus used is illustrated in Fig. 2. The water was driven by a peristaltic pump control velocity into the lower end of the anaerobic reactor. Next, the height difference was produced between the anaerobic reactor and the aerobic reactor. As a result, the effluent from the anaerobic reactor entered the aerobic reactor under the influence of gravity. The anaerobic reactor and the aerobic reactor, with the effective volumes of 2.4 L and 1.2 L, respectively, were both made of Plexiglas [7]. The external diameter of the anaerobic reaction column is 108 mm, the wall thickness is 4 mm, and the height is 1600 mm; the external diameter of the aerobic reaction column is 80 mm, the wall thickness is 4 mm, and the height is 1000 mm. The anaerobic reactor from the bottom up per 200 mm is provided with a water outlet, the setup has a total of 7 outlets, with the highest water outlet being for the anaerobic effluent. The aerobic reactor from the bottom up per 200 mm is provided with a water outlet; set up has a total of 6 outlets, with the final effluent location of coupled system at the top of the water outlet.

2.3. Analysis methods

The COD was measured by using the potassium dichromate method [8]. The ORP was evaluated by using

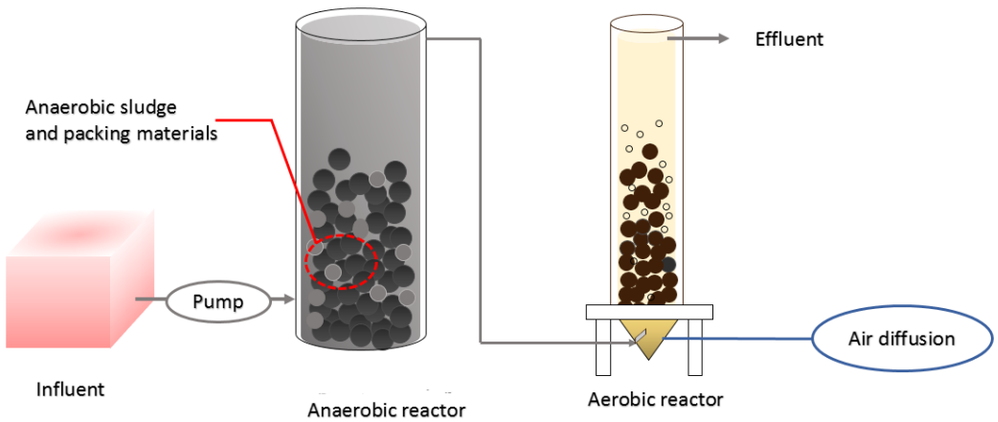

Fig. 2. Flow chart of the test system.

Ray E - 201 - C portable redox potentiometer from Shanghai Precision and Scientific Instrument Corporation. The dye concentration and removal rate were quantitatively determined by UV-Vis[9];the changes of the degradation process and structural component were qualitatively measured based on UV-Vis and Second derivative spectrometry[10].

For the GC-MS analysis, samples for the NIST database were used. The equipment used for the analysis was a Thermo Focus DSQ GC-MS from the US. The samples were first filtered using a centrifugal, and then extracted using a rotary evaporator and a freeze dryer. The third step was the derivatization reaction in the condition of an 85°C oven for 30 min with the addition of 0.1 ml ethyl acetate, 0.1 ml anhydrous and 0.1 ml BSTFA silicon alkylation reagents. 1 μL of each pretreated samples was analysed using the GC-MS system. High purity He gas was used as the carrier gas with a flow rate of 1 ml/min, and splitless sampling was used. The temperature for gasification compartment was maintained at 250°C.

2.4. Experimental result

The optimum technology parameters were: HRT = 7 h, initial pH value = 6, DO = 4 mg·L^{-1}; a strong ability to resist the influence of dye concentration fluctuation was observed in the anaerobic stage of the coupled system. Moreover, the results showed that the concentration of sulphate also affected the removal of organic compounds in the anaerobic stage. As the concentration of sodium sulphate increased, the removal rate of COD in the anaerobic stage was first increased and subsequently decreased at last. When sodium sulphate was not added, the removal rate of COD was 62.4% in the anaerobic stage; the concentration of sodium sulphate in the influent increased to 400 mg/L, and the optimal value of COD removal in the anaerobic stage was 93.6%.When the concentration of sodium sulphate was more than 400 mg/L, as the amount of sodium sulphate increased, the removal rate of the anaerobic stage decreased, and then gradually stabilized. Therefore, the organic substrate degradation of the anaerobic reactor should be considered to occur in two stages.

Under the optimum working conditions, a comparative experiment was conducted on the identical two-stage process using ceramsite as its packing material in the coupled system. During the study, dye removal showed that decolourization mainly occurs in the AF stage. Moreover, microbial decolourization of azo dyes has been widely reported in an anaerobic environment [11].

3. Results and discussion

3.1. Study of the organic degradation kinetics model of the internal electrolytic coupled system

3.1.1. Establishment of the model

Before the matrix degradation kinetics model [12] was deduced, the following assumption were made:

1. The whole system is in steady state.
2. The organic compounds in the influent are dissolved, the influent does not contain insoluble substances, and the influent does not contain microorganisms.
3. According to the homogeneous reactor, the material in the bioreactor is mixed well.
4. The effects of reactive dyes and other substances on the removal of organics and the growth of cells is negligible, and the effect of the internal electrolysis reaction on the removal of organics and the growth of cells is also negligible. The electrochemical reaction is internalized in biochemical reactions, and is considered as a stage of the biochemical treatment strengthening effect.

The model derivation process is shown in Fig. 3:

Using the anaerobic reactor as research object of the system, the formula of the organic materials is given by:

$$Q_0 S_0 = Q_e S_e + \frac{dS_r}{dt} V + \frac{dX}{dt} V \tag{1}$$

In the formula Q_0—Influent flow, L/d; S_r—The concentration of organic substrates in the reactor, mg/L; S_0— The concentration of organics in the influent, mg/L; X—Microorganism concentration in the reactor, mg/L; Q_e— Effluent flow, L/d; V—Effective volume of the anaerobic reactor, L; S_e— The concentration of organics in the effluent, mg/L; $\frac{dS_r}{dt}$ —The rate of organic substrates changes in the reactor, mg/(L·d); $\frac{dX}{dt}$ — The rate of sludge changes in the reactor, mg/(L·d).

From the above model assumptions, we can see that, when the system is stable, the rate of sludge concentration in the reactor does not change and then can be ignored, i.e., $\frac{dX}{dt} = 0$, and the system does not discharge sludge, i.e., $Q_0 = Q_e$.

Thus, the removal rate of organic substrates of the whole anaerobic system is given by:

$$\frac{dS_r}{dt} = \frac{Q_0 (S_0 - S_e)}{V} \tag{2}$$

Defining $t = \frac{V}{Q_0}$ where t is system hydraulic retention time (HRT), we obtain:

$$\frac{dS_r}{dt} = \frac{S_0 - S_e}{t} \tag{3}$$

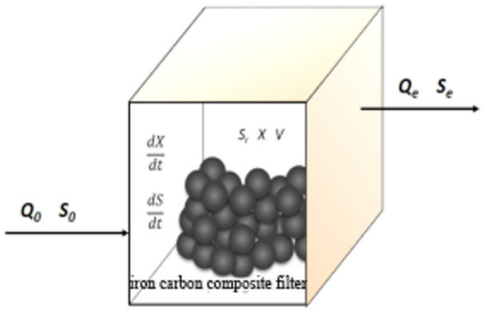

Fig. 3. The anaerobic reactor material balance chart.

It can be seen that, in the non-sludge system, the removal rate of organic substrates is related to the concentration of organic substrates in and out of the water and HRT.

The definition of μ is the removal rate of organic substrates, that is, the amount of microbial removal of organic substrates in the system during unit time:

$$\mu = \frac{1}{X} \times \frac{dS_r}{dt} = \frac{S_0 - S_e}{X \cdot t} \quad (4)$$

In this experiment, the study focus on the degradation process of DW with low organic concentration. Therefore, Eckenfelder model is preferred as the degradation model [13]. The experimental influent conditions meet the substrate concentration conditions of the model that the influent BOD_5 was less than 300 mg/L. In this state, the degradation rate of organic substrates and the residual substrate concentration are presented as a first-order reaction. As a result:

$$\mu = K_2 S_e \quad (5)$$

K_2 is the deceleration growth constant.

Substituting Eq. (5) into the formula Eq. (4) yields:

$$K_2 \cdot S_e = \frac{1}{X} \cdot \frac{dS_r}{dt} = \frac{S_0 - S_e}{X \cdot t} \quad (6)$$

In this experiment, S_0 is a fixed value in the influent, and X is also a constant. By changing the residence time, the concentration S_e of the effluent organics under unvarying conditions was determined. In other words, S_e is taken as the abscissa and μ is taken as the ordinate to obtain the kinetic equations and parameters.

3.1.2 Obtaining the parameters of the kinetic model

1. The concentration of influent COD is 300±20 mg/L, and the dye concentration is 100 mg/L. When sodium sulphate was not added, the degradation of organic in the anaerobic reactor was determined as presented in Table 1:

From Table 1, the kinetic equations can be obtained according to the different HRT and the corresponding concentration of organics in the water.

Using graphical method, the fitting equation is obtained: $y = 0.0027 \quad x - 0.04$, $R^2 = 0.998$. According to Eq. (6), we can see that the slope of the regression curve can be determined as the corresponding K_2, that is, the hydraulic model parameters of the anaerobic reactor ($K_2 = 0.0027$). In conclusion, the kinetic equation of this period is: $\mu = 0.0027 S_e - 0.04$.

2. In the case that the concentration of influent COD is 200±20 mg/L, the dye concentration is 40 mg/L, and sodium sulphate was added at the concentration of 400 mg/L, the degradation of organic in the anaerobic reactor was determined as presented in Table 2:

From Table 2, the kinetic equations can be obtained according to the different HRT and the corresponding concentration of organics in the water.

Using graphical method, the fitting equation is obtained: $\bar{y} = 0.0069 \quad \bar{x} - 0.031$, $R^2 = 0.995$, $K_2 = 0.0069$. In conclusion, the kinetic equation of this period is: $\mu = 0.0069 S_e + 0.031$.

The linear equation and correlation coefficient are obtained by regression line in Fig. 4 and Fig. 5:

Table 1
Organic degradation in the anaerobic reactor

Items	HRT (h)	X (g/L)	S_0 (mg/L)	S_e (mg/L)	$S_0 - S_e$ (mg/L)	μ (1/d)
1	3	5	300	120	180	0.288
2	4	5	280	99	181	0.217
3	5	5	287	86	201	0.193
4	6	5	300	80	220	0.176
5	7	5	300	76	224	0.154

Table 2
Organic degradation in the anaerobic reactor

Items	HRT (h)	X (g/L)	S_0 (mg/L)	S_e (mg/L)	$S_0 - S_e$ (mg/L)	μ (1/d)
1	3	5	200	34	166	0.266
2	4	5	190	25	165	0.198
3	5	5	200	20	180	0.173
4	6	5	200	17	183	0.145

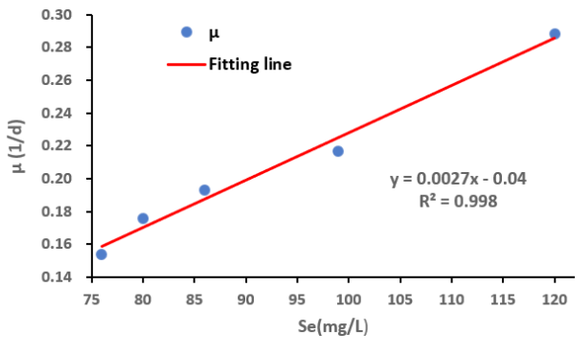

Fig. 4. Fitted line graph.

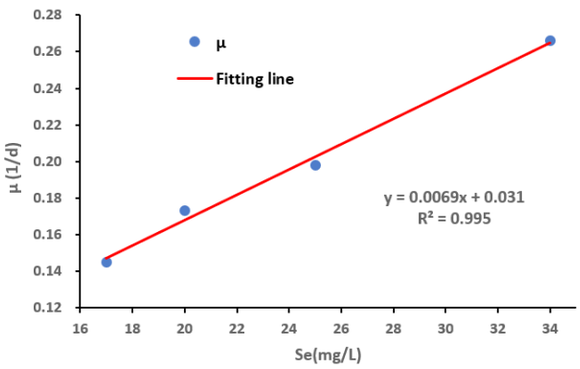

Fig. 5. Fitted line graph.

1) Without adding sulphate:

$$S_e = \frac{S_0 - 14.8}{1 + 0.0027X \cdot t} + 14.8 \quad (7)$$

2) Without adding sulphate:

$$S_e = \frac{S_0 - 4.49}{1 + 0.069} + 4.49 \quad (8)$$

3.1.3 Validation of kinetic equations

To verify the accuracy of the kinetic model, the experimental values and the theoretical values calculated by the kinetic model are listed separately. The theoretical values are calculated using Eqs. (7) and (8).

1. The concentration of influent COD was 300±20 mg/L, the dye concentration is 100 mg/L, without adding sodium sulphate (state 1):
2. The concentration of influent COD was 200±20 mg/L, the dye concentration is 40 mg/L, and sodium sulphate was added at the concentration of 400 mg/L (state 2):

Comparing Table 3 and Table 4, under the condition of state 1, the relative error range between the theoretical values and the experimental values is 2.2%~9.7%,and the maximum absolute error is no more than 8 mg/L; under the condition of state 2, the maximum absolute error between the theoretical values and the experimental values is no more than 6 mg/L, and the relative error value is larger than that of state 1, with the relative error range of 3%~25% because of the small in state 2. In summary, the kinetic equation of the coupled anaerobic reactor derived in this paper can be used for accurate prediction of the experimental results, and the feasibility of the selected model is proved. This study has practical value to estimate the organic substrates of the experimental device within the engineering permissible error range.

3.2. Kinetics analysis of reactive brilliant red X-3B anaerobic degradation

Dye degradation mainly occurs in the anaerobic stage; thus, so based on the removal rules of anaerobic degradation of azo dyes, decolourizaion kinetics of X-3B dyes was investigated in the coupled system anaerobic stage.

In this experiment, the degradation of dye was investigated under the conditions of different dye concentrations of 40 mg/L, 60 mg/L and 80 mg/L while the concentration of influent COD was stable at 200 mg/L and the sodium sulphate concentration was at 400 mg/L. The reactive brilliant red-3B degradation process of the anaerobic biological filter in the coupled bio-electrochemical AF-BAF system follows the first-order kinetic model, which can be expressed as follows:

$$\ln C_i = \ln C_0 - kt \quad (9)$$

In the formula, k is the reaction rate constant; t is the reaction time; C_i is the substrate concentration (mg/L). The fitting figures obtained using the experimental data are shown below.

The fitting results of the first-order kinetic model are shown in Fig. 6 and Table 5, the correlation coefficients of the first-order kinetic are all above 0.97 for each of the three dye concentrations.

According to the first-order kinetic equation that the lower the C_0 is, the greater the value of k will be , i.e., the higher the removal rate of dye. The value of k is directly related to the reactor behaviours and reflects the activity of biomembrane in AF.

From Table 5 we can see that k of the first-order kinetic reaction rate constant did not show a significant decrease

Table 3
The experimental values and the theoretical values of the model in the running process of the system

HRT (h)	Influent (mg/L)	The experimental values of effluent (mg/L)	The theoretical values of effluent (mg/L)	Absolute error (mg/L)	Relative error (%)
3	289	120	117	3	2.5
4	300	95	103	8	8.4
5	302	92	90	2	2.2
6	290	80	78	2	2.2
7	320	85	77	8	9.7

Table 4
The experimental values and the theoretical values of the model in the running process of the system

HRT (h)	Influent (mg/L)	The experimental values of the effluent (mg/L)	The theoretical values of the effluent (mg/L)	Absolute error (mg/L)	Relative error (%)
4	180	29	23	6	20
5	182	24	18	6	25
6	186	20	15	5	25

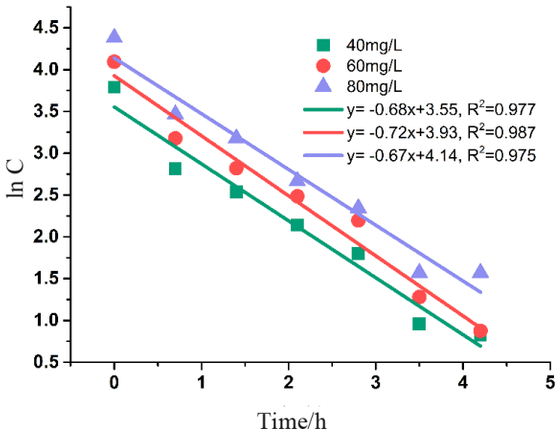

Fig. 6. ln C–t diagram of reactive brilliant red X-3B at different initial dye concentrations.

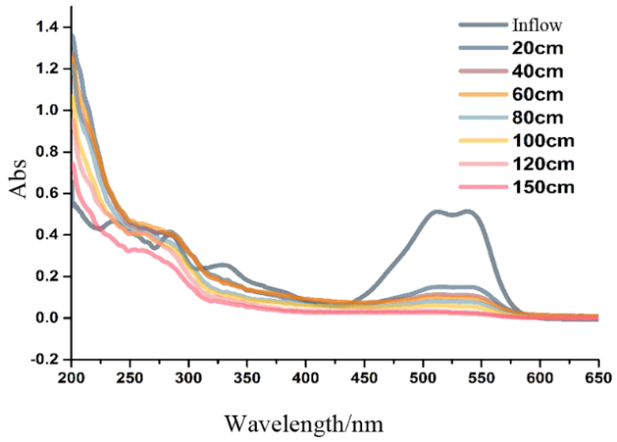

Fig. 7. UV-Vis spectrum of the effluent at different locations of the anaerobic reactor.

Table 5
The anaerobic degradation kinetic parameters of reactive brilliant red X-3B at different initial dyes concentrations

Dye concentration (mg/L)	Kinetic equation	Correlation coefficients R^2	Dye degradation rate constant k
40	ln C = –0.68t + 3.55	0.977	0.68
60	ln C = –0.72t + 3.93	0.987	0.72
80	ln C = –0.67t + 4.14	0.975	0.67

with increase of dye concentration. When the dye concentration is 60 mg/L, the rate constant of the first-order kinetic equation is greater than 40 mg/L. This observation shows that dye degradation in the anaerobic stage is not affected by the initial dye concentration and that the anaerobic reactor has superior resistance to impact load i.e., biofilm has stronger adsorption capacity of dyes. When the dye concentration continues to rise to 80 mg/L, the rate constants of the first-order kinetic equation decrease; this phenomenon may be the result of microorganisms being slightly inhibited under the dye concentration.

3.3. Study of the degradation process of the dye via the coupled bio-electrochemical AF-BAF system

3.3.1. UV-Vis analysis

To investigate the degradation process and structural components of the simulated wastewater with reactive brilliant red-X-3B in the coupled bio-electrochemical AF-BAF system, UV-Vis analysis of the anaerobic and aerobic effluent was conducted. The changes of the material structure in the anaerobic stage were the emphasis of the analysis, because of the decolourization mainly occurs in the anaerobic phase. The changes of the overall dye degradation process were observed in the UV- Vis spectra, as shown in Fig. 7.

Fig. 7 shows that inflow reactive brilliant red-3B have 5 absorption peaks at the wavelength of 236, 285, 330, 512, 539 nm. Moreover, there is a maximum absorption peak in the visible region of 512 nm and 539 nm. Based on the molecular structure of X-3B, the absorption peak of the conjugate system formed by azo bonds is analysed; the inflow in the ultraviolet region has three absorption peaks at 236 nm, 330 nm and 285 nm, which have been identified as benzene ring, naphthalene ring and three triazine, respectively.

Fig. 7 also reflects dye degradation of effluent at different locations of the reactor. In the visible spectral region (>400 nm), the peak intensity decreases gradually with the increase of reactor height (the residence time is prolonged) and the characteristic absorption peak almost disappeared at the height of 120 cm from the bottom of reactor;, the disappearance of the characteristic absorption peak is caused by the breaking of the conjugated chromophore of azo double bond. In addition, Fig. 6 shows that the dye degradation dynamics of the reactor are significant at the beginning of the process. Subsequently, the removal kinetics of the dye decreases over time. Thus, the first-order kinetic model of the dye degradation process was verified.

The change of dye degradation in the ultraviolet region(>400 nm) was observed, as shown in Fig. 8.

Fig. 8 shows that the three characteristic absorption peaks of the benzene ring, naphthalene and triazine are all located in the ultraviolet region. The figure shows that the benzene ring, naphthalene ring and three triazine groups were destroyed and that ring-opening occurred. The absorbance in the wavelength range of 200~250 nm was greatly increased. According to the law of conservation of mass, some small molecule compounds have been produced that only absorb in the ultraviolet region [14]. At the heights in the range of 40–60 cm from the bottom of the anaerobic reactor, the absorbance in the wavelength range of 200~300 nm increases as the height of the reactor increases. It is assumed that the dye is degraded into benzene and the structure of the benzene ring may be formed when the naphthalene ring structure is destroyed. Therefore, the structure of the benzene ring begins to accumulate gradually.

When the reactor height is greater than 80 cm, the absorbance of effluent is obviously lower than that of the previous stage in the wavelength range of 200~300 nm. This

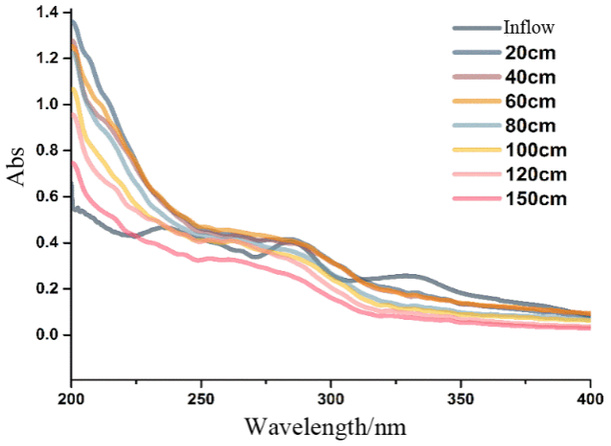

Fig. 8. UV-Vis spectrum of the effluent at different locations of the anaerobic reactor.

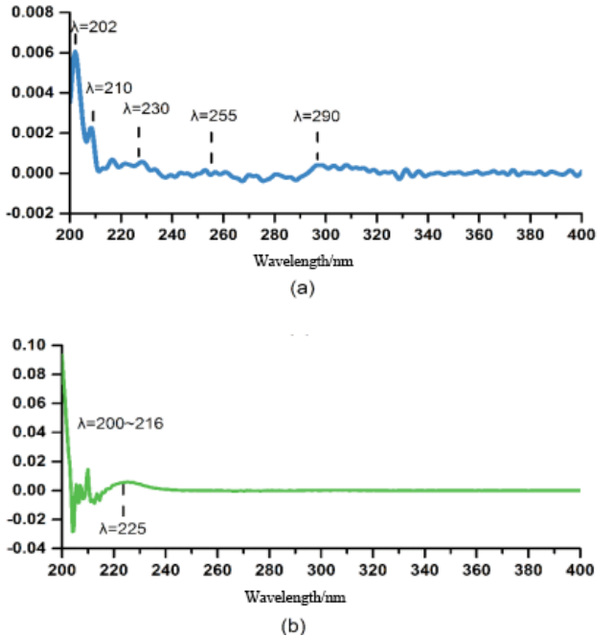

Fig. 9. two second-derivative spectra of the effluent at each stage:(a) anaerobic effluent;(b)aerobic effluent.

phenomenon can be explained as follows: the coupled anaerobic reactor rapidly degrades X-3B azo dyes, and the upper layer of anaerobic reactor continuously degrades the intermediate products of a relatively small molecular weight; mineralization may even be possible in the wavelength range of 200–300 nm.

The use of derivative spectra have some advantages: eliminating background interference, enhancing fine structures of spectra and identifying complex spectra. Therefore, the second-derivative spectra of anaerobic and aerobic effluent are shown in Figs. 9a and 9b, to distinguish the overlapped peaks or the absorption peaks concealed by the rapid change of absorbance.

The two second derivative spectra of the anaerobic effluent show that weak absorptions remain at the wavelengths of 202 nm, 210 nm, 230 nm, 255 nm and 290 nm in the ultraviolet region. As shown in Fig. 9a, absorption peaks exist at both 202 nm and 255 nm; these peaks correspond to the absorption band [9] of the benzene ring structure. The peak intensity is obvious at 202 nm; according to the nature of influent, and the characteristics of anaerobic, unsaturated compounds, such as acetic acid and propionic acid, are deduced (their absorption bands are approximately 200 nm). The absorption band with a certain intensity indicates that the absorption band may have a fine structure of the benzene ring or naphthalene ring in the range wavelength of 255~300 nm. Azo conjugated structures obtained by the reductive degradation produce aromatic amines, such as aniline compounds. Their two characteristic absorption peaks of aromatic amines are located at approximately 230 nm and 280 nm, indicating that the increase in dye concentration can inhibit the activity of microorganisms. It is caused by the intermediate products of dye degradation, such as aromatic amines, which can be toxic to microorganisms, and intermediate products usually produce more toxicity than the dye itself. A slight inhibitory effect of the microorganisms of the system is found under this dye concentration. The two second-derivative spectra of the aerobic effluent are shown in Fig. 9b. There is no absorption peak at the wavelengths greater than 240 nm. This observation indicated that the structure of the benzene ring and naphthalene ring have significantly changed after processing at this stage in the anaerobic effluent, and that the absorption peak of aniline has disappeared. The peak positions of the two second-derivative spectra are mainly located at wavelengths less than 200~210 nm, and the peak intensity is very large; the wastewater is found to mainly contains unsaturated bond compounds (such as alcohols, ethers and esters, acids and other small molecules) according to the nature of water.

As a result of the above analysis, we have a definite understanding based on the material structure that the process of the coupled system for degradation of reactive brilliant red-3B dye molecules. The anaerobic stage destroys azo chromophores, which obviously leads to the decolourization from the initial reaction. The naphthalene ring structure, the three triazine structure and the benzene ring structure were somehow destroyed, as indicated by the spectra in the ultraviolet region, and the coupled system had more power to degrade the naphthalene ring structure. Naphthalene rings may be degraded into small molecules that contain substituted benzene rings, and the azo conjugated structures can be reduced and cleaved to produce aromatic amines, such as aniline. When the wavelength is 200~250 nm, the absorbance appears to be first increased and then decreased, that is, the process of reactive brilliant red-3B degradation produces the benzene derivatives or intermediate products of small molecules containing unsaturated bonds. At the beginning of the reaction, the benzene derivatives or small molecules gradually accumulate first in the lower part of the reactor, and then the middle and upper layers start to degrade. It is demonstrated that the internal electrolysis packing can play a coupling role in AF and strengthen the degradation ability of the intermediates of the benzene ring and naphthalene ring in the anaerobic

Table 6
Products of the anaerobic effluent

Peak	R.T. (min)	Products	Chemical structural formula
1	4.54	Ethylene glycol	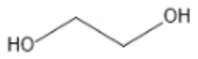
2	4.78	Glycolic acid	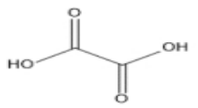
3.	5.12	Lactic acid	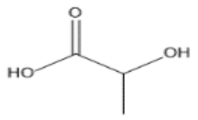
4	6.31	Propylene glycol	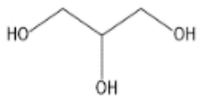
5	7.03	6-hydroxyhexic acid	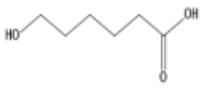
6	6.48	Benzene acetic acid	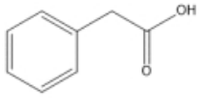
7	7.22	cumene	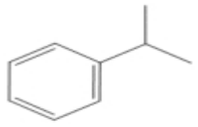

stage. The remaining benzene ring derivatives were further degraded by the subsequent aerobic stage. Finally, the system effluent is mainly small molecules containing unsaturated bonds.

3.3.2. GC-MS analysis

To infer the degradation process according to the degradation products obtained from the reactive brilliant red-3B via the coupled system, while ensuring the biodegradability and toxicity of products at the same time, the end products in the effluent of each stage are tested, the products obtained are shown in Tables 6 and 7.

The Table 6 shows that, after the anaerobic process, reactive brilliant red-3B mainly produces acids and alcohols, including glycerol, ethylene glycol, glycolic acid, and lactic acid. There is a low concentration of intermediate products having the benzene ring structure, such as benzene acetic acid and cumene, and no intermediary products containing naphthalene ring structure are detected in the anaerobic effluent. All the above information suggests that the structure of naphthalene rings may have been degraded into benzene rings in the reaction. In addition, aniline was not detected in the UV-Vis analysis. The results indicate that the coupling removal of reactive brilliant red-3B is very thorough in the anaerobic stage and can realize partial degradation of naphthalene and aromatic amines.

Table 7
Products of the aerobic effluent

Peak	R.T (min)	Products	Chemical structural formula
1	4.54	Ethylene glycol	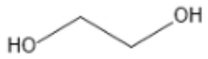
2	5.12	Lactic acid	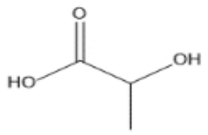
3	6.31	Propylene glycol	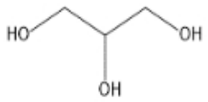
4	7.03	6-hydroxyhexic acid	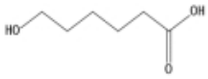

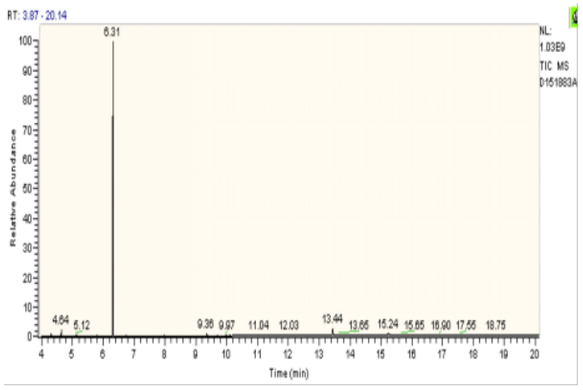

Fig. 10. GC-MS of the anaerobic effluent

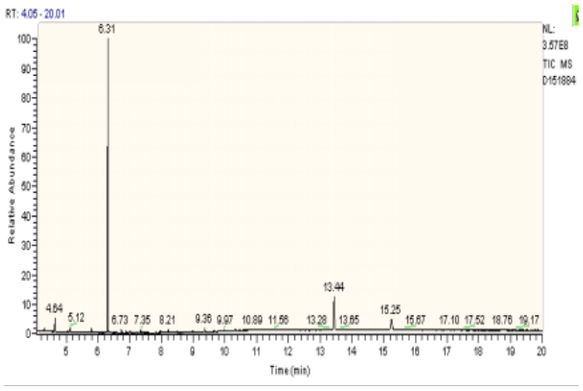

Fig. 11. GC-MS of the aerobic effluent.

After the effluent of the anaerobic stage passed through the aerobic stage, the benzene ring material was further degraded and removed. Finally the effluent was found to only contain lactic acid, glycolic acid, propylene glycol and 6-hydroxyhexic acid, as shown in Table 7.

3.3.3. Reactive brilliant red -3B degradation process

According to the above analysis and results of GC-MS and UV-Vis, the degradation process of reactive brilliant red-3B in the coupled system was deduced to be as follows. First, azo dyes under anaerobic conditions with zero-valent iron as an electron donor release electrons that attack $-N=N-$ key, resulting in its fracture and form amino hydroxy aniline and naphthalene compounds. Second, these two intermediate products can be further degraded to phenylacetic acid, glycolic acid, glycol and all forms of alcohols, acids and other organic substances in the internal electrolysis coupled anaerobic effluent. Some aniline are converted to phenol under specific anaerobic conditions, and the benzene ring of phenol is interrupted and converted to simple organic compounds, such as 6-hydroxy caproic acid. Under aerobic conditions, benzene compounds of the anaerobic stage are further degraded to small molecules with unsaturated bonds. In addition, the ORP was maintained at approximately –220 mV in the anaerobic reactor, and gas generation was observed on the surface of anaerobic pool. It was speculated that some organic compounds had been transformed into CH_4 or fully mineralized to CO_2 and H_2O in this environment. Moreover, the influent organic components are single and more glycerin ingredients can be found in the anaerobic and aerobic effluents; thus, microorganisms may be reduced by using other triose produced by hexose as hydrogen receptors in the anaerobic reaction process [15].

In summary, the degradation process of reactive brilliant red-3B in the coupled system is shown in Fig. 12.

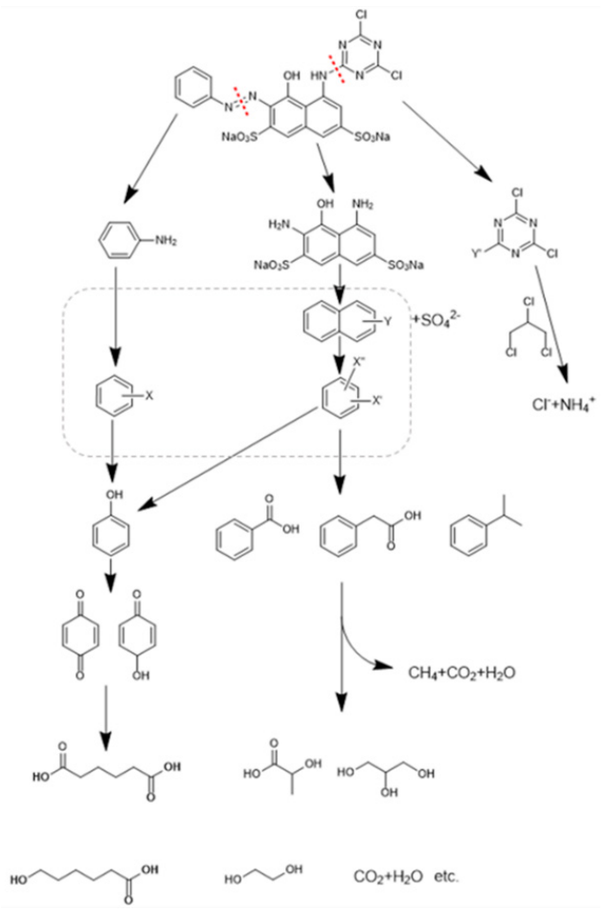

Fig. 12. Degradation process of reactive brilliant red-3B in the coupled bio-electrochemical AF-BAF.

4. Conclusions

A novel coupled system is established by iron-carbon inner electrolysis combined with AF-BAF for the treatment of dyeing wastewater. The experimental results show that the degradation rate of organic substrates and the residual substrate concentration follow a first-order reaction based on the Eckenfelder model, which is used as the organic degradation kinetic model. Moreover, the reactive brilliant red-3B degradation process of the anaerobic stage was found to follow the first-order kinetic model in the coupled system.

According to the results of UV-Vis and GC-MS, the internal electrolysis packing can destroys the azo chromophore. After being treated by the coupled system, most of the intermediate products are reduced and the products in the final effluent are mainly composed of small molecules containing unsaturated bonds.

Acknowledgement

The authors would like to acknowledge the financial support from the National Science Foundation of China (Nos.20676079), the National Science and Technological Foundation of China (Nos.2006BAJO4A09)

References

[1] Y.N. Lee, G.Y. Nan, X.M. Dai, Research status and development trends of technologies for dyeing wastewater advanced treatment in china, J. HE. Arch. Civil. Eng., 34(02) (2016) 69–72.
[2] Z.M. Yang, Overview of physicochemical treatment for printing and dyeing wastewater, Textile Dye. Finish. J., 37(12) (2015) 45–51.
[3] B.E.L. Baêta, D.R.S. Lima, S.Q. Silva, S.F Aquino, Evaluation of soluble microbial products and aromatic amines accumulation during a combined anaerobic/aerobic treatment of a model azo dye, Chem. Eng. J., 259 (2015) 936–944.
[4] L.H. Huang, G.P. Sun, T. Yang, B. Zhang, Y. He, X.H. Wang, A preliminary study of anaerobic treatment coupled with micro-electrolysis for anthraquinone dye wastewater, Desalination, 309 (2013) 91–96.
[5] S. Tsuneda, T. Ohno, K. Soejima, A Hirata, Simultaneous nitrogen and phosphorus removal using denitrifying phosphate-accumulating organisms in a sequencing batch reactor, Biochem. Eng. J, 3(27) (2006) 191–196.
[6] Tongji University, Preparation of iron-carbon microelectrolysis filler, China: 200910198816.9,2010-05-12.
[7] M.Q. Yang, Research on new technique of microbial electrochemical coupling with anaerobic/aerobic degrading the wastewater from cotton dyeing pretreatment, 2017.
[8] The original state environmental protection administration "Water and Wastewater monitoring and analysis method" editorial board, Water & Wastewater Monitoring and Analysis, 4th ed., Beijing: China Environmental Science Press, 2002: 35–106.
[9] H. Zhang, Modern organic spectral analysis, Beijing: Chemical Industry Press, 2005. 186–202.

[10] Z.SH. Lee, Advanced analysis and test technology, Harbin: Harbin Engineering University Press, 2005. 165–172.
[11] F.Y. Kong, A.J. Wang, H.Y. Ren, Improved azo dye decolorization in an advanced integrated system of bioelectrochemical module with surrounding electrode deployment and anaerobic sludge reactor, Biores. Technol., 175 (2015) 624–628.
[12] ZH.B. Chen, ZH.Q. Chen, N.Q. Ren, H.CH. Wang, SH.K Nie, M.H. Cui, Modeling of mixed liquor inorganic suspended solids and membrane flux at different ratio of SRT to HRT in a submerged membrane bioreactor, Appl. Math. Model, 36(1) (2011) 173–182.
[13] G.Z.H. Tang, Analytic solution of Eckenfelder model in microbial deceleration growth, CN. Water. Wastewater, 15(5) (1999) 58–59.
[14] C.H.M. Huang, Study on Bio-decolorization of Azo dyes and Biodegration of its Intermediates Anilines, Guangzhou: South China University of Technology, 2012.
[15] W.Q. Qi, Microbial production of glycerol and research process, Tech. Inno. Appl., 30(5) (2013) 43.